Food Chemistry 464 (2025) 141890

Contents lists available at ScienceDirect

Food Chemistry

journal homepage: www.elsevier.com/locate/foodchem

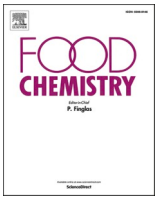

Mechanism of maltogenic α-amylase modification on barley granular starches spanning the full range of amylose

Li Ding [a], Wenxin Liang [a], Staffan Persson [a,b], Sylwia Głazowska [a], Jacob Judas Kain Kirkensgaard [c,d], Bekzod Khakimov [c], Kasper Enemark-Rasmussen [e], Kim Henrik Hebelstrup [f,g], Andreas Blennow [a,g,*], Yuyue Zhong [a,h,*]

[a] Copenhagen Plant Science Center, Department of Plant and Environmental Sciences, Faculty of Science, University of Copenhagen, Denmark
[b] Joint International Research Laboratory of Metabolic & Developmental Sciences, State Key Laboratory of Hybrid Rice, SJTU-University of Adelaide Joint Centre for Agriculture and Health, School of Life Sciences and Biotechnology, Shanghai Jiao Tong University, Shanghai, China
[c] Department of Food Science, University of Copenhagen, DK-1958 Frederiksberg C, Denmark
[d] Niels Bohr Institute, University of Copenhagen, DK-2100, Copenhagen Ø, Denmark
[e] Department of Chemistry, Technical University of Denmark, DK-2800, Kemitorvet, Building 207 Kgs. Lyngby, Denmark
[f] Department of Agroecology, Aarhus University, Flakkebjerg, Denmark
[g] PlantCarb Aps, Hørsholm, Denmark
[h] Department of Food Science and Nutrition, The Hong Kong Polytechnic University, Hung Hom, Kowloon, Hong Kong, China

ARTICLE INFO

Keywords:
Amylose
Barley
Maltogenic α-amylase
Hydrolysis
Degree of branching

ABSTRACT

Amylopectin (AP)-only (APBS), normal (NBS), and amylose (AM) only (AOBS) barley starches were selected here to investigate catalysis pattern of maltogenic α-amylase (MA) on hydrolyzing AP and AM granular starches. MA shortened starch side chains with degree of polymerization (DP) 11–30. MA-treated APBS exhibited porous granular structures and dramatically increased degree of branching (DB, 17–20 %), and reduced ordered degrees, suggesting high hydrolysis and transglycosylation activities of MA. MA-treated NBS showed less pronounced porous structures and slightly increased DB (2–4 %), indicating high hydrolysis but low transglycosylation activities. AOBS displayed minimal changes in DB (0.2–0.3 %) and starch structures, implying low hydrolysis and transglycosylation activities. Therefore, MA preferred to attack the AP molecules with abundant glucan substrates with DP 11–30, while AM restricted MA activity likely by creating ineffective binding sites and undergoing rapid reorganization. These findings deepened the understanding of the mechanisms of MA in modifying granular starches with varying AM content.

1. Introduction

Starch is one of the most predominant carbohydrates found in practically all green plant organs and tissues. It is also an essential raw material for different industrial sectors, including food, paper, bioplastic production, and drug delivery (Fox, 2018; Laycock & Halley, 2014; Luallen, 2018; Wurzburg, 1972). The industrial utilization of starch typically requires pre-treatments and modifications to overcome various inherent shortcomings of native starches, such as fast retrogradation, low water solubility, and poor resistance to high temperatures (Maniglia, Castanha, Le-Bail, Le-Bail, & Augusto, 2021; Zhong et al., 2022). Enzymatic pre-treatment is an efficient, mild, and eco-friendly method increasingly utilized in modifying starch (Li et al., 2022a).

Maltogenic α-amylase (MA, glucan 1,4-α-maltohydrolase, EC 3.2.1.133), belonging to the glycoside hydrolase family 13 (GH13), is particularly interesting in enzymatic modification due to its dual hydrolase activity: *exo*-glucanase and *endo*-glucanase activity (Keeratiburana, Hansen, Soontaranon, Blennow, & Tongta, 2020; Zhong, Keeratiburana, et al., 2021). This enzyme typically exhibits exo-activity to randomly hydrolyze α-1-4 glycosidic bonds, releasing α-maltose from the non-reducing end. In addition, MA also shows high transglycosylation activity to form α-1,6 linkages when substrates contain maltooligosaccharide segments (Zhong, Xu, et al., 2022). The multi-functionality of MA has resulted in numerous applications for

* Corresponding author at: Copenhagen Plant Science Center, Department of Plant and Environmental Sciences, Faculty of Science, University of Copenhagen, Denmark.
E-mail addresses: ab@plantcarb.com (A. Blennow), yuyuezhong93@163.com (Y. Zhong).

https://doi.org/10.1016/j.foodchem.2024.141890
Received 28 August 2024; Received in revised form 27 October 2024; Accepted 30 October 2024
Available online 2 November 2024

efficient granular starch modification, making it more effective compared to non-hydrolyzing transglycosylation enzymes: (i) increasing the branching degree and reducing the retrogradation rate of starch molecules, thereby commonly utilized in the baking sector as an anti-staling agent (Chen et al., 2020; Grewal et al., 2015); (ii) developing porous starch materials (Keeratiburana et al., 2020); (iii) increasing the specific surface area of starch granules, thereby improving the catalytic efficiency of subsequently used glucosyltransferases, such as starch branching enzymes and transglucosidases (Zhong et al., 2021; Zhong, Keeratiburana, et al., 2021).

Starch is primarily organized by two macromolecules: linear amylose (AM) and branched amylopectin (AP). Increasing AM content (AC) was reported to significantly reduce the catalysis efficiency of MA in three maize starches with AC of 3.3 %, 29.9 % and 68.6 %, respectively (Li et al., 2022b). However, the reason for higher MA resistance of granular starches with increasing AC is still unclear, as the hybrid of AP and AM molecules in these starches complicated the understanding of MA's catalytic pattern and activity. To address this issue, pure AM and pure AP granular starches serve as good model materials for studying MA's behavior. While pure AP starches have been found in various crops, such as maize, barley, and potato, pure AM starch has only been reported in barley, specifically in the so-called AM-only starch (AOBS) (Carciofi et al., 2012). AOBS is characterized by a high degree of granular irregularity and aggregation, a rough surface, and low levels of crystalline and lamellar order, as reported in (Tian et al., 2024). Given the significant differences in the molecular structures and functional roles of AP and AM in the granular architecture, we hypothesize that MA exhibits distinct catalytic characteristics when interacting with pure AM versus pure AP granular starches.

In the present study, pure AP, pure AM, and hybrid barley starches were utilized in their granular forms to investigate the catalytic patterns of MA. The three starches were treated with MA at two different enzyme concentrations, and subsequent changes in their molecular, helical, crystalline, and granular structures, as well as their thermal properties were analyzed. The results of this study will enhance our understanding of MA's catalytic behavior on AM and AP molecules within their granular states.

2. Materials and methods

2.1. Materials

AP-only barley starch (APBS, cv. Cinnamon) was obtained from Lantmännen SW Seed, Sweden. Normal barley starch (NBS, cv. Golden Promise) and AM-only barley starch (AOBS), generated in the Golden Promise genetic background (Carciofi et al., 2012), were kindly provided by plantCarb ApS, Hørsholm, Denmark. Maltogenic α-amylase (23,000 U/mL) was kindly supplied by Novozymes (Bagsvaerd, Denmark). Pancreatin from porcine pancreas (Cat. No. P7545, activity 8 × USP) and amyloglucosidase (Cat. No. A7095, activity 300 units / mL) were bought from Sigma-Aldrich (St. Louis, MO, USA), while isoamylase (*E*-ISAMY, 200 units / mL) was purchased from Megazyme (K-TSTA, Megazyme, Co. Wicklow, Ireland). All other chemicals used in this study were of reagent grade obtained from reliable suppliers.

2.2. Enzymatic modification

MA-treated barley starches were prepared with method described by Zhong, Keeratiburana, et al. (2021). Starch (2 g) was suspended in 40 mL of 50 mM sodium acetate buffer (pH 5.5) containing 5 mM calcium chloride, and the starch suspension was then incubated at 50 °C for 10 min for starch swelling. Two concentrations of MA, low (L-MA, 2300 U) or high (H-MA, 11500 U), were added to the starch samples, and incubated at 40 °C for 6 h for enzymatic modification. Then, 1 M sodium hydroxide solution was added dropwise until the pH of the starch solution was 11, and another 10-min incubation at 40 °C was done to stop the enzyme reaction. Finally, 1 M hydrochloric acid solution was added to adjust the pH to 6.0, followed by washing thrice with MilliQ water, centrifugation to remove residual salts and lyophilization. Control samples for each type of starch (buffer treated) were prepared following the same procedure without adding an MA solution. A detailed summary of the samples and treatments employed in this study is presented in Table 1.

2.3. Chain length distribution (CLD) and apparent amylose content (AAC)

A high-performance anion exchange chromatography-pulsed amperometric detection system (HPAEC-PED, Dionex, Sunnyvale, CA, USA) was employed to analyze the distribution of chain length. Briefly, 5 mg of starch was suspended in 1 mL of 100 mM acetate buffer (pH 4.0). The full gelatinization of starch samples was achieved by heating at 99 °C for APBS and NBS sample or at 130 °C for AOBS sample for one hour with manually shaking every 10 mins. The obtained starch paste was debranched through a three-hour-incubation at 40 °C with 0.4 U isoamylase under the 500 rpm of shaking, and another ten-minute-incubation at 99 °C was done to deactivate the enzyme. Finally, 40 μL of the debranched supernatant was injected into a CarboPac PA-200 column at a flow rate of 0.4 mL per minute. The program for running the samples was as described in (Tian, Liu, et al., 2024).

The AAC of all samples was measured using iodine colorimetry as described in (Tian, Liu, et al., 2024).

2.4. Degree of branching (DB)

A 600 MHz nuclear magnetic resonance (NMR) spectrometer (Bruker Avance III; Bruker Biospin, Rheinstetten, Germany) was applied to acquire the one-dimensional ^{1}H NMR spectral data (Zhong, Keeratiburana, et al., 2021). The preparation procedures of starch solutions (5 mg/mL) were: firstly, fully gelatinized in D_2O at 99 °C (APBS and NBS samples) or 130 °C (AOBS samples) for 2 h and lyophilized; secondly, redissolved in 9:1 (*v*/v) DMSO (containing 1 mg/mL 3-(Trimethylsilyl) propionic-2, 2, 3, 3-d 4 acid sodium salt (TSP)) and D_2O at 99 °C for 30 min. Finally, the one-dimensional ^{1}H signal NMR spectroscopy of the obtained starch solution were collected at 60 °C, and the resonances of anomeric protons corresponding to α 1,4- (5.2 ppm) and α 1,6-glucosidic (4.8 ppm) linkages of starch samples were evaluated using SigMa (Khakimov,

Table 1
The overview of the experiment design, apparent amylose content (AAC) and degree of branching (DB) for native, buffer- and MA-treated APBS, NBS and AOBS samples[1].

Samples codes[2]	Acetate buffer	MA	AAC (%)	DB (%)
APBS	no	no	1.2 ± 0.1^{a}	7.3 ± 0.6^{b}
APBS-buffer	yes	no	1.3 ± 0.1^{a}	7.1 ± 0.5^{b}
APBS-L-MA	yes	1150 U/g	1.2 ± 0.1^{a}	24.9 ± 1.4^{a}
APBS-H-MA	yes	5750 U/g	1.0 ± 0.1^{a}	27.3 ± 7.1^{a}
NBS	no	no	29.0 ± 0.3^{c}	3.0 ± 0.2^{b}
NBS-buffer	yes	no	36.4 ± 2.0^{a}	3.3 ± 0.1^{b}
NBS-L-MA	yes	1150 U/g	32.7 ± 0.8^{b}	5.5 ± 0.3^{a}
NBS-H-MA	yes	5750 U/g	31.1 ± 1.1^{bc}	7.3 ± 3.3^{a}
AOBS	no	no	99.8 ± 1.2^{a}	1.3 ± 0.3^{a}
AOBS-buffer	yes	no	83.0 ± 2.7^{b}	1.3 ± 0.1^{a}
AOBS-L-MA	yes	1150 U/g	83.6 ± 4.6^{b}	1.5 ± 0.1^{a}
AOBS-H-MA	yes	5750 U/g	82.7 ± 1.1^{b}	1.6 ± 0.1^{a}

[1] Values are means ± SD. Values with different letters in the same column are significantly different at $p < 0.05$.

[2] APBS, amylopectin-only barley starch; NBS, normal barley starch; AOBS, amylose-only barley starch; buffer, samples incubated only with buffer solution; L-MA, samples treated with the low concentration of maltogenic α-amylase; H-MA, samples treated with the high concentration of maltogenic α-amylase. The sample codes presented in this Table are used consistently in the following tables.

Mobaraki, Trimigno, Aru, & Engelsen, 2020). The DB values were determined using the eq. 1.

$$DB(\%) = \frac{\alpha-1,6 \text{ linkage peak area}}{\alpha-1,6 \text{ linkage peal area} + \alpha-1,4 \text{ linkage peak area}} \times 100 \quad (1)$$

2.5. Helical structures

The helical structures of MA-treated starch samples were analyzed using a solid-state ^{13}C NMR spectrometer (Bruker AV-600) at a ^{13}C frequency of 150.9 MHz, with the same setting parameters described in our previous report (Ding et al., 2023). Amorphous references of barley starches were prepared by fully gelatinization of APBS suspensions (1 % *w/v*) in MilliQ water for 1 h at 99 °C, followed by snap freezing in liquid nitrogen and lyophilization.

2.6. Crystalline structures

The crystalline structures of starch samples were analyzed by a Nano-inXider instrument (Xenocs SAS, Grenoble, France) equipped with a Cu Kα source with a 1.54 Å wavelength and a two-detector setup, with the same setting parameters described in our previous report (Ding et al., 2023). The crystalline peak was fitted and analyzed by PeakFit 4.0 (Systat Software Inc., San Jose, CA, USA). The total, V-type (2θ at 7°, 13° and 20°), A- (APBS and NBS) or B- (AOBS) type relative crystallinities were calculated using the eq. 2, eq. 3 and eq. 4, respectively.

$$\textit{Total relative crystallinity}\ (\%) = \frac{\textit{Crystalline peak area}}{\textit{total}\ \text{diffraction}\ \textit{area}} \times 100 \quad (2)$$

$$\textit{V\_type crystallinity}\ (\%) = \frac{\textit{V\_type crystalline peak area}}{\textit{total}\ \text{diffraction}\ \textit{area}} \times 100 \quad (3)$$

$$\textit{A\_/B\_type crystallinity}\ (\%) = \textit{Total crystallinity} - \textit{V\_type crystallinity} \quad (4)$$

2.7. Short-range order

A MB100 Fourier Transform Infrared (FTIR) spectrometer (ABB-Bomem, Quebec, Canada) was used to analyze starch short-range order bonding structure. Sixty-four scans were applied for each starch sample from 4000 to 500 cm^{-1} at a resolution of 8 cm^{-1} with background air. The deconvolution of each FTIR spectrum spanning from 1200 to 800 cm^{-1} was achievedusing OMNIC 8.0 (Thermo Fisher Scientific Inc., Madison, WI) with a half-bandwidth of 19 cm^{-1} and an enhancement factor of 1.9 (Wang, Wang, Guo, Liu, & Wang, 2017). The short-range ordered structure was characterized by calculating the ratios of absorbance values at 1047 to 1022 cm^{-1}.

2.8. Granular structures

Field Emission Scanning Electron Microscopy (FE-SEM, FEI Quanta 200) was used to visualize the granular topography and morphology. The starch samples were imaged at an acceleration voltage of 10 kV at 2500× and 10,000× magnification after fixing and gold sputter coating.

2.9. Thermal properties

The thermal parameters of MA-treated samples were measured by a differential scanning calorimeter 1 (Mettler Toledo, Schwerzenbach, Switzerland). Starch (8 mg) were weighed into standard aluminium (APBS and NBS samples) or medium-pressure stainless-steel crucibles (AOBS samples), and then 15 μL of MilliQ water was added, followed by seal and equilibration at 4 °C overnight. The pans were heated from 30 to 120 °C (APBS and NBS samples) or to 180 °C (AOBS samples) with a heating rate of 10 °C per minute using an empty pan as reference.

2.10. Statistical analysis

All experiments were conducted at least in three replicates, and the results were presented as means ± standard deviations. For ^{13}C NMR, one measurement was performed. Statistically significant differences ($p < 0.05$) were analyzed by Analysis of Variance (ANOVA) followed by Duncan's test using SPSS 25.0 software (SPSS, Inc. Chicago, IL, USA).

3. Results

3.1. Effects of MA treatment on the AAC, DB and CLD

The starch samples utilized in this study exhibited a wide range of distinct AAC: 1.2 % for APBS, 29.0 % for NBS, and 99.8 % for AOBS (Table 1), indicating their AP-only, hybrid of AP and AM, and AM-only characteristics, respectively. Buffer incubation only (no MA) increased the AAC of NBS to 36.4 %, decreased that of AOBS to 83.0 %, and had little effect on the APBS. Low concentrations of MA treatment significantly reduced the AAC of NBS by 3.7 % compared to buffer control, while further increases in MA concentration had no significant effect (Table 1). A similar decrease in AAC upon MA treatment was reported for rice starch (Keeratiburana et al., 2020) and pulse starches (Li, Li, Zhu, & Ai, 2021). However, the AAC of AOBS remained unaffected by MA treatment, even under high MA concentrations. Neither buffer nor MA treatments significantly impacted the AAC of APBS, which is in line with a previous study (Li et al., 2022a).

The ^{1}H NMR spectra of the gelatinized starch samples revealed two peaks (Fig. S1) at 4.8 and 5.2 ppm that corresponded to the anomeric protons of α-1,6 and α-1,4 linkages, respectively (Ding et al., 2023). The DB values in Table 1 indicated that APBS, consisting of virtually pure AP, displayed the highest DB (7.3 %), followed by NBS (3 %), and AOBS had the lowest DB, 1.3 %. Buffer treatment did not significantly affect the DB values in any of the tested samples, while high-concentration MA treatment increased the DB in APBS and NBS by 20.2 % and 4 %, respectively. The increased DB for the two starch samples is likely attributed to *exo*-α-1,4-glucanase and/or transglycosylation activities of MA, which are higher in APBS than in NBS. Interestingly, no significant effect of MA on the DB was observed for AOBS, even at high MA concentration, likely due to minor MA activity.

CLD profiles of debranched starches (Fig. 1), analyzed by HPAEC-PAD, showed that buffer treatment had little effect on the CLD of branched starches, consistent with previous report (Zhong, Herburger, et al., 2021). While, MA treatment with low-concentration shifted the CLD in APBS (Fig. 1A) and NBS towards shorter chains (Fig. 1B), which indicates a typical exo-α-1,4-glucanase activity of MA to attack the exterior chains of AP. A relative increase in branches with DP 2–10 was observed in those samples, accompanied by a reduction in the relative contents of AP chains with DP ≥ 11 in APBS (Fig. 1D) and DP 11–30 in NBS (Fig. 1E). This suggested that MA probably targeted the AP chains with DP 11–30. MA is also shown to target the AP side chains with DP ≥ 12 of waxy maize (Grewal et al., 2015), DP 10–30 for normal maize (Zhong, Keeratiburana, et al., 2021) and DP 10–40 for normal wheat starches (Zhai, Li, Bai, Jin, & Svensson, 2022). The CLD for MA-treated AOBS showed a decline in AM side chains with DP 8–22 and an increase in AM side chains with DP 2–6 (Fig. 1F), indicating that side chains with DP 8–22 were likely the primary substrates of MA for an AM-only starch sample. It is noteworthy that MA modification slightly increased the contents of AM side chains with DP 22–57 in AOBS, indicating the limited *endo*-α-1,4-glucanase activity of MA on longer AM chains (Leman, Goesaert, Vandeputte, Lagrain, & Delcour, 2005). In this case, a slight increase in the side chains with DP 30–40 in NBS likely indicated an endo-α-1,4-glucanase activity of MA on AM chains rather than on AP chains. Increased concentration of MA slightly shifted the CLDs towards shorter chains in NBS, while the effect was less prominent for pure AP (APBS) or AM (AOBS) samples.

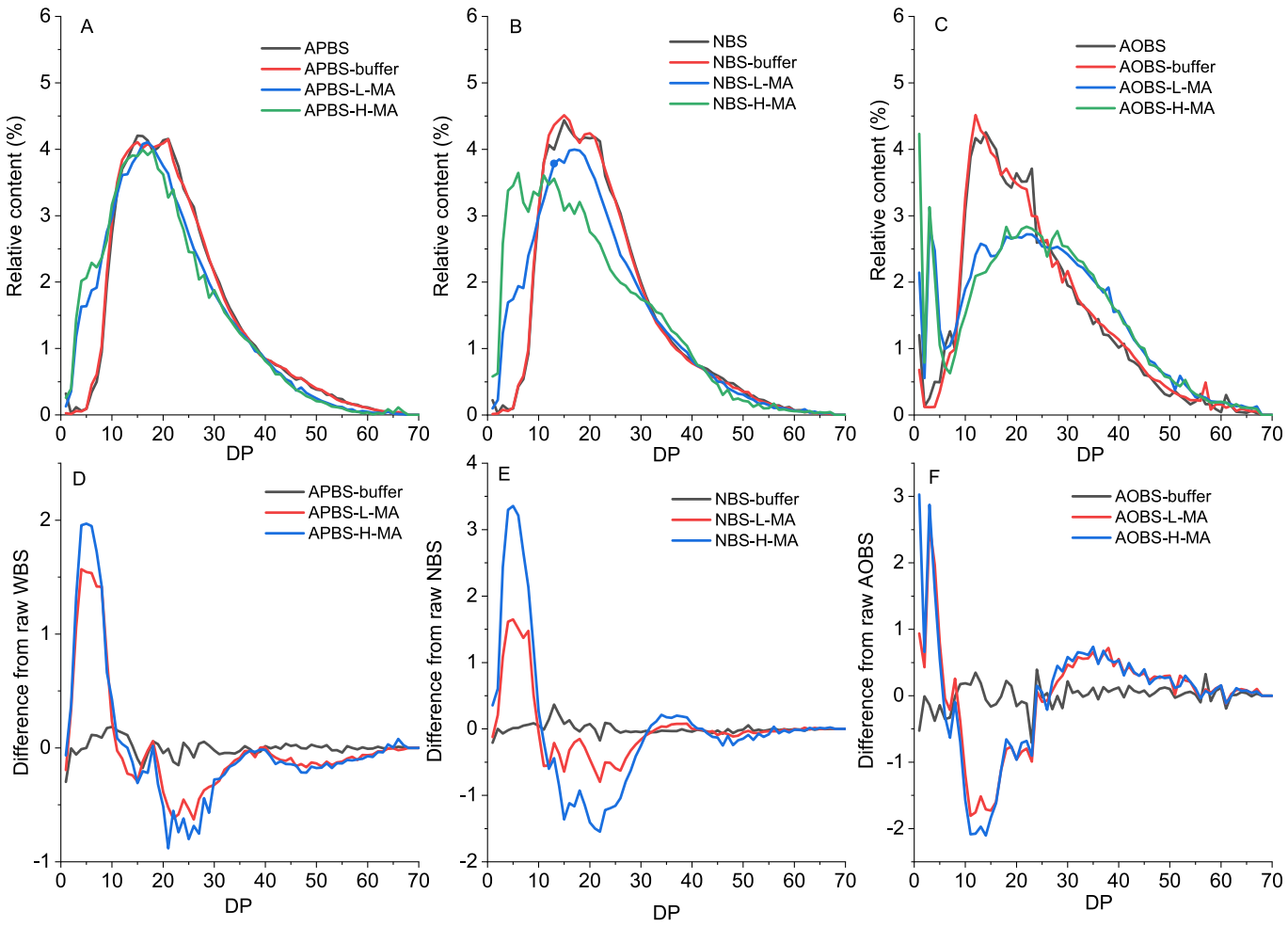

Fig. 1. Chain length distributions (A, B and C) of debranched native, buffer- and MA-treated APBS, NBS and AOBS samples, and their distribution difference plots from corresponding native controls (D, E and F) (APBS, amylopectin-only barley starch; NBS, normal barley starch; AOBS, amylose-only barley starch; buffer, samples incubated only with buffer solution; L-MA, samples treated with the low concentration of maltogenic α-amylase; H-MA, samples treated with the high concentration of maltogenic α-amylase).

Table 2
The relative contents of double-helical, single-helical and amorphous regions obtained by ^{13}C NMR analysis, A/B/V-type crystallinity measured by WAXS and the ratio at 1047/1022 cm^{-1} calculated from the FTIR spectra for native, buffer- and MA-treated APBS, NBS and AOBS samples[1].

Samples	^{13}C NMR			WAXS				FTIR ratio at 1047/1022 cm^{-1}
	Double helix (%)	Single helix (%)	Amorphous region (%)	A-type crystallinity (%)	B-type crystallinity (%)	V-type crystallinity (%)	Total crystallinity (%)	
APBS	35.0	n.d.[2]	65.0	35.4 ± 0.7^{a}	n.d.	0.6 ± 0.0^{a}	36.0 ± 0.7^{a}	0.78 ± 0.01^{a}
APBS-buffer	27.0	n.d.	73.0	25.9 ± 0.3^{b}	n.d.	0.6 ± 0.0^{a}	26.5 ± 0.3^{b}	0.67 ± 0.02^{b}
APBS-L-MA	22.0	n.d.	78.0	16.0 ± 1.5^{c}	n.d.	0.5 ± 0.0^{a}	16.6 ± 1.5^{c}	0.60 ± 0.01^{c}
APBS-H-MA	25.0	n.d.	75.0	16.1 ± 0.9^{c}	n.d.	0.5 ± 0.0^{a}	16.6 ± 0.9^{c}	0.60 ± 0.01^{c}
NBS	33.8	11.3	55.0	23.1 ± 1.2^{a}	n.d.	1.9 ± 0.4^{a}	25.0 ± 1.4^{a}	0.66 ± 0.01^{a}
NBS-buffer	22.3	5.7	72.0	16.2 ± 1.3^{b}	n.d.	1.9 ± 0.1^{a}	18.1 ± 1.4^{b}	0.57 ± 0.00^{b}
NBS-L-MA	13.9	11.1	75.0	15.0 ± 1.1^{b}	n.d.	1.9 ± 0.2^{a}	16.9 ± 0.9^{b}	0.56 ± 0.00^{b}
NBS-H-MA	15.0	10.0	75.0	14.6 ± 0.7^{b}	n.d.	1.7 ± 0.2^{a}	16.3 ± 0.8^{b}	0.55 ± 0.00^{b}
AOBS	5.6	22.4	72.0	n.d.	5.3 ± 0.6^{a}	6.2 ± 1.2^{a}	11.2 ± 1.8^{a}	0.54 ± 0.00^{a}
AOBS-buffer	5.6	22.4	72.0	n.d.	2.6 ± 0.9^{b}	5.7 ± 0.5^{ab}	8.3 ± 0.4^{b}	0.47 ± 0.00^{c}
AOBS-L-MA	5.8	23.2	71.0	n.d.	2.2 ± 0.4^{b}	5.0 ± 0.8^{b}	7.2 ± 0.4^{b}	0.49 ± 0.01^{b}
AOBS-H-MA	5.2	20.8	74.0	n.d.	2.3 ± 0.0^{b}	5.5 ± 0.1^{ab}	7.9 ± 0.1^{b}	0.50 ± 0.01^{b}

[1] Values are means ± SD. Values with different letters in the same column are significantly different at $p < 0.05$.
[2] n.d. = not detectable.

3.2. Effects of MA treatment on the starch helical and crystalline structures

The relative contents of double and single helices, and amorphous regions of starches extracted from ^{13}C NMR spectra (Fig. S2) showed that APBS mainly had double helices, while NBS and AOBS were mixtures of both types of helices with double helices predominantly found in NBS and single helices in AOBS (Table 2) (Liang et al., 2023). Buffer treatment decreased double helix content in APBS and NBS by 8 % and 11.5 %, respectively. Low-concentration MA treatment further reduced the double helix content of APBS and NBS by 5 % and 8.4 %, respectively, compared to the buffer controls, but a further increase in the enzyme concentration did not affect the double helix content (Table 2). The decreased double helices were attributed to the typical *exo*-α-1,4-glucanase activity of MA. This activity shortened the AP side chains with DP 11–30, which build the crystalline nano-lamellae by forming double helices in starch granules (Bertoft, 2017), thereby decreasing the double helical content. Only minor effects of either buffer or MA treatments on the contents of double and single helices in the AOBS sample indicate that this type of starch is highly resistant to the MA treatment under the conditions used (Table 2).

WAXS profiles (Fig. 2) showed that the NBS and APBS samples displayed a typical A-type allomorph, whereas the AOBS displayed a combination of B-type and V-type allomorph as reported (Liang et al., 2021; Zhong et al., 2021). V-type allomorph is attributed to single helices formed by AM and endogenous lipids. The native APBS had the highest total crystallinity, followed by NBS and AOBS (Table 2), while the order for the V-type crystallinity was the opposite. These data demonstrated that increased AAC resulted in less ordered crystalline structures but more AM-lipid single helices (Zhong, Li, et al., 2021). Buffer incubation or enzymatic modification did not change the crystalline patterns. Significant decreases in A-type crystallinity were observed in buffer-treated APBS (by approx.10 %) and NBS (by approx. 7 %) compared to the native samples, consistent with their decreased double helix content (Table 2). The incubation of AOBS granules in buffer solution led to a 2.7 % of reduction in B-type crystallinity, indicating that buffer incubation decreased the level of long-range order by disrupting the arrangement of double helices in AOBS without affecting the total amount of helices (unchanged helical structure in Table 2). MA treatment led to a further significant decrease (by 10 %) in the A-type crystallinity of the APBS, perhaps suggesting that this enzyme mainly attacked the double helices (formed by the side chains with DP 11–30) in the crystalline regions of the AP-only starch. While, no significant changes in the crystallinity were observed for MA-treated NBS and AOBS, even at high concentrations. Combined with the decreased double helix content data of MA-treated NBS, MA possibly simultaneously disrupted the double helices in crystalline region as defects and non-registered ones in the amorphous region of this hybrid starch, thereby showing no change in the crystallinity. For AOBS, no change in crystallinity is probably attributed to the low activity of MA on AM-only starch.

3.3. Effects of MA treatment on the starch granular structures

The FTIR spectral 1047/1022 cm^{-1} ratios were measured to indicate the short-range molecular order on the granule surface, as the bands centered at 1047 and 1022 cm^{-1} are sensitive to changes in the crystalline and amorphous regions, respectively (Kizil, Irudayaraj, & Seetharaman, 2002). APBS exhibited the highest surface short-range molecular order, followed by NBS and AOBS, consistent with their relative content of double helices and crystallinity (Table 2). Buffer incubation significantly decreased the ratios at 1047/1022 cm^{-1} for all starch types. A low concentration of MA treatment reduced the ratio in APBS compared to the buffer control, and increasing the concentration of MA had no further effect on the spectral ratio. However, MA treatment did not affect the ratio in NBS, regardless of enzyme concentration, consistent with no change in the crystallinity. Interestingly, MA-treated AOBS showed a significant increase in the 1047/1022 cm^{-1} ratio, indicating a more ordered granular structure caused by reorganization of AM molecules with high mobility.

Granular morphology visualized by SEM (Fig. 3) indicated that native APBS and NBS exhibited both large and small granules in round shape with smooth surface (Song & Jane, 2000), while a high level of irregularity, aggregation and rough surface were observed for native

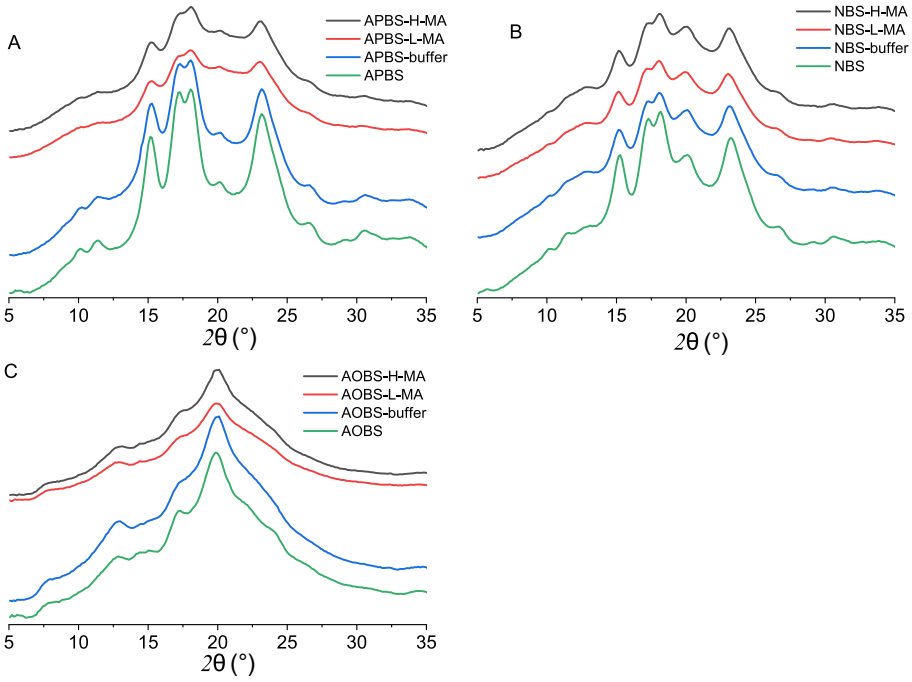

Fig. 2. Wide angle X-ray scattering (WAXS) diffractograms of native, buffer- and MA-treated APBS (A), NBS (B), and AOBS (C) samples (All abbreviations are the same as in Fig. 1).

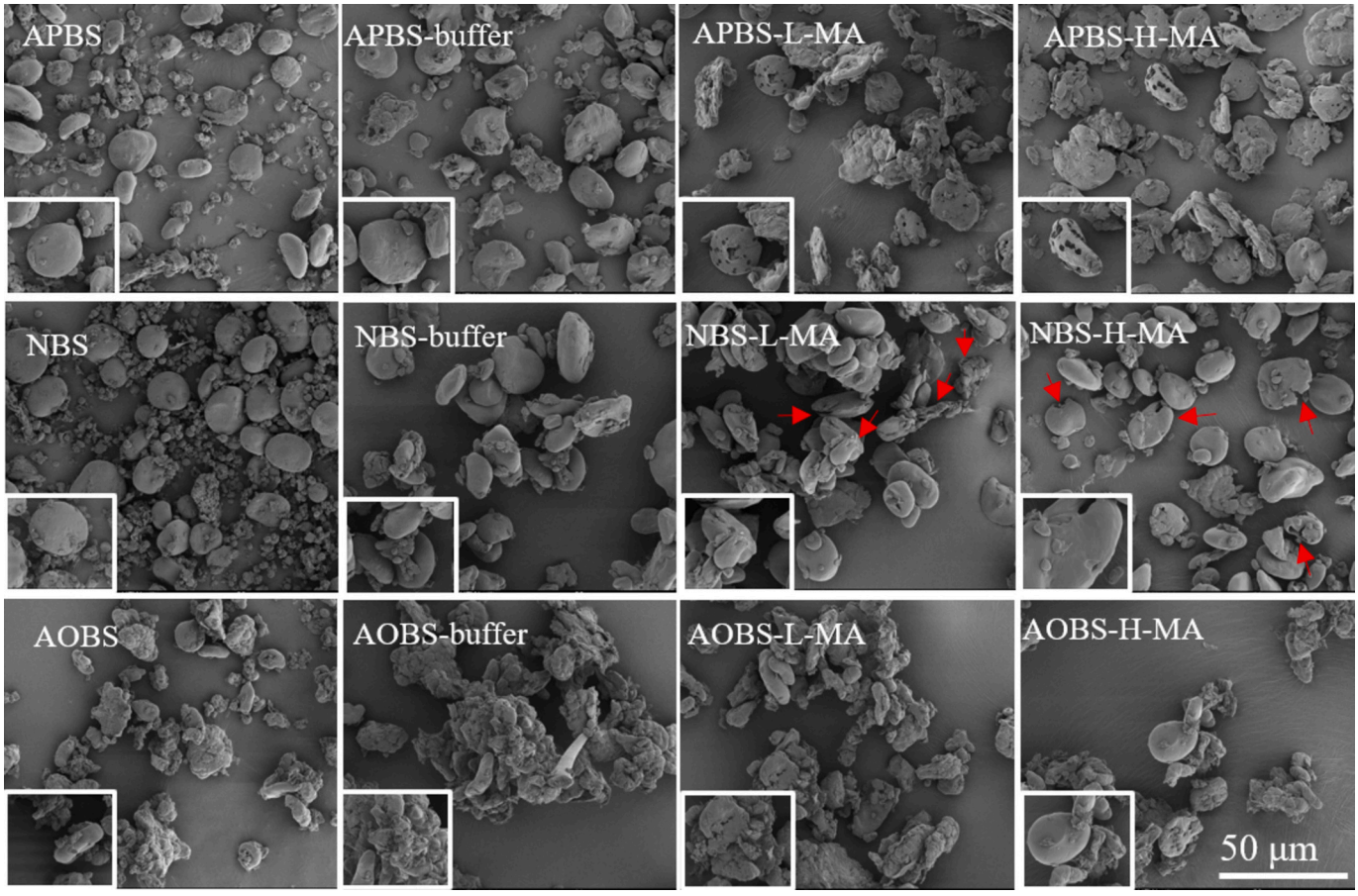

Fig. 3. Scanning electron microscopy (SEM) of native, buffer- and MA-treated APBS, NBS and AOBS samples (All abbreviations are the same as in Fig. 1; Arrows indicate the cracks and broken granules).

AOBS (Tian, Liu, et al., 2024). After treatment with MA, low concentration produced numerous pores and inner channels in APBS, with higher concentration generating deeper pores and channels. While, MA treatment of NBS induced peripheral cracks and broken granules at low concentrations, and an increased concentration led to more cracks and broken granules (Fig. 3, Arrows). However, no apparent changes were found for MA-treated of AOBS, even under high concentrations of MA treatment. This demonstrated the highest enzymatic resistance of AM-only starch and explained its unchanged helical and crystalline structures after MA treatment (Table 2) (Zhong et al., 2022).

3.4. Effects of MA treatment on the starch thermal property

The thermal parameters, including the thermal stability (T_o, T_p and T_c), crystallite heterogeneity (ΔT) and amount (ΔH), of the native, buffer-treated, and MA-treated APBS, NBS, and AOBS samples, are summarized in Table 3. APBS and NBS exhibited lower T_o, T_p, T_c, and ΔT values but higher ΔH values than AOBS. These results suggested that AOBS has fewer crystallites with higher thermal stability and greater heterogeneity than APBS and NBS (Tian, Liu, et al., 2024). Buffer incubation reduced the heat stability of the crystallites (lower T_o, T_p, and T_c) and the crystallite amount (lower ΔH), but increased the degree of heterogeneity (higher ΔT) in APBS and NBS. Notably, buffer incubation increased T_o, and decreased T_c and ΔT in AOBS. MA treatment further reduced the crystallite amount of APBS and NBS, but had no effect on AOBS, consistent with the changes in their double helical structures (Table 2). In addition, less uniform crystallites (higher ΔT) were formed in MA-treated APBS compared to buffer control. While, AOBS showed more stable (increased T_o, T_p, and T_c) and more homogenous (decreased ΔT) crystallites after MA treatment, further implying the high reorganization ability of AM molecules. MA-treated NBS showed no significant differences in T_o, T_p, T_c, and ΔT, suggesting no change in the thermal stability and degree of heterogeneity of its starch crystals.

4. Discussion

4.1. Buffer incubation without enzyme addition is an essential control in enzyme modification of granular starches

Acetate buffer solutions are frequently employed to maintain the optimal pH for targeted enzymes during the enzymatic modification of starch (Liu, Antoniou, Li, Ma, & Zhong, 2015). However, in many related studies, the control conditions often involve raw starches, with the impact of the buffer itself, where starch is incubated without enzymes, being overlooked. In this study, it was observed that buffer incubation alone led to significant changes in AAC, helical structure, crystalline and granular surface short-range order, and thermal properties of all barley starches, as detailed in the Results section. Our previous research also indicated that buffer controls notably affected the structure of maize starches (Zhong, Keeratiburana, et al., 2021). Therefore, it is crucial to recognize that buffer controls can have a significant impact on granular starches. Without incorporating a buffer control, directly comparing raw starch with enzyme-modified starch may yield misleading conclusions, as it becomes challenging to discern whether the observed differences are due to the buffer or the enzyme treatment.

Our findings indicated that buffer control primarily induced a disordering effect on the helical, crystalline, and surface short-range order.

Table 3
Thermal properties of native, buffer- and MA-treated APBS, NBS and AOBS samples[1]

Samples	T_o[2] (°C)	T_p[2] (°C)	T_c[2] (°C)	ΔT[2] (°C)	ΔH[2] (J/g)
APBS	58.5 ± 0.4[a]	64.9 ± 0.2[a]	74.2 ± 0.4[a]	15.7	7.4 ± 0.7[a]
APBS-buffer	54.2 ± 0.1[b]	62.9 ± 0.0[b]	71.7 ± 0.5[b]	17.5	6.6 ± 0.1[b]
APBS-L-MA	50.7 ± 2.2[c]	62.9 ± 0.9[b]	71.3 ± 0.0[b]	20.6	4.1 ± 0.4[c]
APBS-H-MA	52.3 ± 1.1[bc]	63.4 ± 1.8[ab]	71.8 ± 1.2[b]	19.5	3.2 ± 0.2[d]
NBS	56.9 ± 0.0[a]	62.9 ± 0.1[a]	70.7 ± 0.3[a]	13.8	7.2 ± 0.0[a]
NBS-buffer	52.0 ± 0.1[b]	60.7 ± 0.4[b]	69.1 ± 0.5[ab]	17.1	4.6 ± 0.1[b]
NBS-L-MA	53.3 ± 0.9[b]	61.1 ± 1.0[ab]	68.4 ± 0.4[b]	15.1	3.4 ± 0.3[c]
NBS-H-MA	52.5 ± 0.6[b]	61.7 ± 1.5[ab]	69.5 ± 1.8[ab]	17.0	3.4 ± 0.1[c]
AOBS	75.3 ± 0.0[c]	95.4 ± 0.2[b]	111.5 ± 0.5[a]	36.2	2.5 ± 0.4[a]
AOBS-buffer	83.0 ± 0.4[b]	95.1 ± 0.0[b]	104.6 ± 0.1[c]	21.6	2.2 ± 0.1[a]
AOBS-L-MA	87.2 ± 0.1[a]	96.8 ± 0.2[b]	104.7 ± 0.3[c]	17.5	2.3 ± 0.0[a]
AOBS-H-MA	89.3 ± 0.5[a]	98.7 ± 0.1[a]	106.9 ± 1.0[b]	17.6	2.5 ± 0.2[a]

[1] Values are means ± SD. Values with different letters in the same column are significantly different at $p < 0.05$.
[2] T_o, onset gelatinization temperature; T_p, peak gelatinization temperature; T_c, conclusion gelatinization temperature; ΔT, T_c-T_o, melting temperature range; ΔH, enthalpy change.

One of the reasons for this phenomenon is the low pH of the buffer (pH 5.5). Previous studies have demonstrated that the pasting properties of maize starch significantly decreased when treated with sulfite salts at pH levels ranging from 2.8 to 5.7 (Yang et al., 2005). Therefore, the weak acidic environment (pH 5.5) likely disrupted the hydrogen bonds within the starch granules, thereby weakening the molecular interactions and unwinding the double helices. These changes further disrupted the ordered structures, and ultimately lowered the stability of starch granules. Additionally, prolonged penetration of water molecules in the acetate buffer may have led to granule swelling and structural loosening, exacerbating the disordering effect of the acidic pH on starch granular stability. The second reason might be the ionic effect of acetate ions and hydrogen ions in the acetate buffer, which might slightly interact with the hydroxyl groups on the starch molecules. This interaction probably altered the charge distribution and increased electrostatic repulsion between starch molecules, leading to granule swelling and further structural disorder (Golachowski et al., 2015).

Except for the disordering effects on the ordered structures of all barley starches, buffer control also increased the AAC of NBS as measured using the iodine binding method. This is perhaps attributed to the hydrolytic effect of the buffer on AM molecules, which increased the number of AM fragments capable of binding iodine. However, buffer control remarkably decreased the AAC of AOBS. This decrease could be due to the lower molecular weight (Mw) of AM in AOBS compared to NBS (Carciofi et al., 2012). Consequently, the hydrolysis of AM in AOBS produced shorter AM fragments with a reduced capacity for iodine binding (Zhong, Tian, et al., 2021). However, the exact mechanisms underlying the effects of buffer incubation on the AAC remained to be investigated in the future. It is also worth mentioning that the ΔT of APBS and NBS increased in buffer control, while the opposite phenomenon was observed in AOBS. APBS and NBS are AP and double helix-rich starches with highly ordered crystalline architecture. The disruption of some double helices by the buffer likely resulted in less uniform crystalline structures, leading to a broader ΔT. Conversely, AOBS, rich in AM and single helices, has a more disordered crystalline structure. Buffer control likely removed the most unstable crystals with low melting temperatures, thereby elevating the onset gelatinization temperature and resulting in a narrower ΔT.

4.2. MA showed high catalytic efficiency on short glucan chains with DP 11–30

A previous study reported that increasing AAC resulted in lower MA catalytic efficiency in maize starches (Li et al., 2022b). Our study found similar results in barley starches, further suggesting that decreasing MA efficiency with increasing AAC applied to both maize and barley starches. This phenomenon is consistent with the understanding that starch with higher AAC exhibits greater resistance to enzymatic reaction, likely due to reduced efficient binding sites (Tian et al., 2024). At a relatively low enzyme concentration of 52 U/g, MA was shown to exhibit a high transglucosylation activity in normal maize starch, with the DB value increasing by 3.7 % (Zhong, Keeratiburana, et al., 2021). However, our preliminary experiments indicated that at 52 U/g of enzyme concentration, the DB in NBS remained almost unchanged (data not shown). Only when the MA concentration exceeded 500 U/g, an increase in its DB was observed. These observations suggested that barley starches had higher enzymatic resistance than maize starches, and thus MA exhibited lower transglucosylation activity in NBS compared to normal maize starch. Moreover, in the literature comparing the effects of MA on maize starches with varying AAC, only <1 % of increases in DB were found in waxy and normal maize starches when using an enzyme activity of 11 MANU/g (Li et al., 2022a). This increase is considerably lower than the 3.7 % observed in normal maize starch in our previous study (Zhong, Keeratiburana, et al., 2021). Direct comparisons are challenging due to differences in enzyme source, enzyme unit, buffer conditions, incubation temperatures, and durations across studies. It can be simply concluded that in their experimental system, MA primarily exhibited high hydrolysis activity with minimal transglucosylation. However, in our system, MA demonstrated both significant hydrolysis and transglucosylation activities. Therefore, these findings of this study provided a clearer understanding of catalytic patterns of MA on pure AM and AP molecules in the granular state.

Notably, a 17 %–20 % increase in DB value (Table 1) and a porous granular structure (Fig. 3) were observed in APBS. The result indicated that MA exhibited both high hydrolysis and transglucosylation activities on AP molecules. However, only a 2 % - 4 % increase in DB was found in NBS, despite of a noticeable porous structure. This suggested that the presence of AM significantly limited the transglucosylation activity of MA. This phenomenon was further confirmed in AOBS with only a 0.2 % - 0.3 % increase in DB and no porous structure. These results imply that MA had an extremely low catalytic efficiency on AM molecules. While, the decreased relative amount of AM side chains with DP 8–22 (Fig. 1 C and F) in MA-treated AOBS provided evidence that MA efficiently hydrolyzed the AM molecules. AM molecules in AOBS demonstrated a strong reorganization ability during hydrolysis (Liang et al., 2023). This was well supported by the increased surface short-range order (Table 2) and thermal stability (Table 3) of MA-treated AOBS in our study. Thus, it is suggested that MA efficiently hydrolyzed AM molecules only in the initial stage, and then the cleaved AM molecules rapidly reorganized, thereby resisting further transglucosylation by MA.

Another interesting observation was that MA greatly increased the relative content of short side chains with DP < 10 by decreasing the proportion of medium side chains with DP 11–30 across all three starches. This indicated that MA preferentially attacks glucans with chain lengths of DP 11–30. Therefore, the high catalytic efficiency in APBS and the low catalytic efficiency in AOBS were likely due to the greater abundance of side chains with DP 11–30 in AP molecules compared to AM molecules, as supported by the DB data (Table 1, 7.3 % vs 1.3 %). MA largely attacked and disrupted these DP 11–30 chains in APBS, which are the main components of double helices and crystalline

nano-lamellae (Bertoft, 2017). Hence, its double helices and structural order significantly reduced (Table 2), leading to decreased amount of less uniform crystallites (Table 3). While, minor activity of MA on these side chains for the AM-only starch led to no significant changes in the helical and crystalline structures in AOBS. However, the abundance of side chains with DP 11–30 did not fully explain the significant lower catalytic efficiency of MA on AP molecules in NBS compared to these in APBS, as NBS is also an AP-rich starch with 3.0 % of DB. A recent enzymatic catalysis study showed that the high enzymatic resistance of glucoamylase on AM molecules is attributed to that the enzyme readily binds to AM molecules but struggles to form enzyme-substrate complexes for further efficient catalysis (Tian et al., 2023). In other words, AM molecules had numerous ineffective binding sites and limited attacking sites. It appears that a similar phenomenon was also applied in MA enzyme as well. In NBS, AM molecules are more flexible compared to AP molecules, as they do not contribute to the granular architecture like AP does. This flexibility may facilitate AM's binding to MA but restrict the formation of enzyme-substrate complexes, thereby in turn decreasing the amount of MA binding to AP chains and significantly reducing the catalytic efficiency of MA. Thus, similar to APBS, MA also attacked the side chains with DP 11–30 in NBS, leading to decreased double helices. However, no change in the crystallinity, short-range order and thermal stability implied that these disrupted double helices by MA for this hybrid starch were in both crystalline (crystalline defects) and amorphous regions (non-registered helices).

5. Conclusion

Three different types of granular barley starches with a full range of AAC (1 %, 29 %, and 100 %) were treated with MA to investigate how MA catalyzed AM and AP molecules in the granular state. Our study firstly emphasized the importance of buffer control in enzymatic modification studies on granular starches, as the buffer incubation alone significantly disordered the structures of starch granules. Secondly, MA exhibited high hydrolysis and transglucosylation activities on AP molecules, perhaps due to their enriched amounts of side chains with DP 11–30, which are preferred substrates of MA in the granular state. AM molecules limited both the hydrolysis and transglucosylation activities of MA, likely by creating numerous ineffective binding sites and undergoing rapid reorganization during hydrolysis. The study further demonstrated that AP was the preferred substrate of MA, due to its enriched amounts of side chains with DP 11–30. This provides insights for optimizing MA modification of starches in their granular state. Notably, MA was found to generate a new type of AP molecule by increasing the DB value from 7.3 % to 27.3 %, a phenomenon previously unreported. This novel finding could offer new functionalities for starches in various industrial applications, including improved thickening agents, production of slowly digestible food products, extended shelf life of bakery items, enhanced stability in food products, and innovative materials for biodegradable packaging.

CRediT authorship contribution statement

Li Ding: Writing – original draft, Validation, Software, Methodology, Investigation, Conceptualization. **Wenxin Liang:** Software, Methodology, Investigation. **Staffan Persson:** Writing – review & editing. **Sylwia Głazowska:** Conceptualization. **Jacob Judas Kain Kirkensgaard:** Writing – review & editing, Methodology. **Bekzod Khakimov:** Writing – review & editing, Methodology. **Kasper Enemark-Rasmussen:** Writing – review & editing, Methodology. **Kim Henrik Hebelstrup:** Resources. **Andreas Blennow:** Writing – review & editing, Supervision, Resources, Conceptualization. **Yuyue Zhong:** Writing – review & editing, Writing – original draft, Supervision, Resources, Project administration, Conceptualization.

Declaration of competing interest

The authors declare that they have no known competing financial interests or personal relationships that could have appeared to influence the work reported in this paper.

Acknowledgement

Li Ding wants to thank the China Scholarship Council funding (CSC, 202006150028) supporting her PhD study at the University of Copenhagen, Denmark. Staffan Persson was funded by Danish National Research Foundation (DNRF155), a Villum (25915) and two Novo Nordisk grants (19OC0056076 and 20OC0060564). Wide angle X-ray scattering data was produced by the research infrastructure in the department of food science at the University of Copenhagen, partly funded by FOODHAY (Food and Health Open Innovation Laboratory, Danish Roadmap for Research Infrastructure).

Appendix A. Supplementary data

Supplementary data to this article can be found online at https://doi.org/10.1016/j.foodchem.2024.141890.

Data availability

Data will be made available on request.

References

Bertoft, E. (2017). Understanding Starch Structure: Recent Progress. *Agronomy, 7*(3), 56.
Carciofi, M., Blennow, A., Jensen, S. L., Shaik, S. S., Henriksen, A., Buléon, A., … Hebelstrup, K. H. (2012). Concerted suppression of all starch branching enzyme genes in barley produces amylose-only starch granules. *BMC Plant Biology, 12*(1), 223.
Chen, X., Zhang, L., Li, X., Qiao, Y., Zhang, Y., Zhao, Y., Chen, J., Ye, X., Huang, Y., Li, Z., & Cui, Z. (2020). Impact of maltogenic alpha-amylase on the structure of potato starch and its retrogradation properties. *International Journal of Biological Macromolecules, 145*, 325–331.
Ding, L., Liang, W., Qu, J., Persson, S., Liu, X., Herburger, K., … Zhong, Y. (2023). Effects of natural starch-phosphate monoester content on the multi-scale structures of potato starches. *Carbohydrate Polymers, 310*, Article 120740.
Fox, G. (2018). Chapter 16 - starch in brewing applications. In M. Sjöö, & L. Nilsson (Eds.), *Starch in food (second edition)* (pp. 633–659). Woodhead Publishing.
Golachowski, A., Zieba, T., Kapelko-Zeberska, M., Drozdz, W., Gryszkin, A., & Grzechac, M. (2015). Current research addressing starch acetylation. *Food Chemistry, 176*, 350–356.
Grewal, N., Faubion, J., Feng, G., Kaufman, R. C., Wilson, J. D., & Shi, Y. C. (2015). Structure of waxy maize starch hydrolyzed by Maltogenic alpha-amylase in relation to its Retrogradation. *Journal of Agricultural and Food Chemistry, 63*(16), 4196–4201.
Keeratiburana, T., Hansen, A. R., Soontaranon, S., Blennow, A., & Tongta, S. (2020). Porous high amylose rice starch modified by amyloglucosidase and maltogenic alpha-amylase. *Carbohydrate Polymers, 230*, Article 115611.
Khakimov, B., Mobaraki, N., Trimigno, A., Aru, V., & Engelsen, S. B. (2020). Signature mapping (SigMa): An efficient approach for processing complex human urine (1)H NMR metabolomics data. *Analytica Chimica Acta, 1108*, 142–151.
Kizil, R., Irudayaraj, J., & Seetharaman, K. (2002). Characterization of irradiated starches by using FT-Raman and FTIR spectroscopy. *Journal of Agricultural and Food Chemistry, 50*(14), 3912–3918.
Laycock, B. G., & Halley, P. J. (2014). Chapter 14 - starch applications: State of market and new trends. In P. J. Halley, & L. Avérous (Eds.), *Starch polymers* (pp. 381–419). Amsterdam: Elsevier.
Leman, P., Goesaert, H., Vandeputte, G., Lagrain, B., & Delcour, J. (2005). Maltogenic amylase has a non-typical impact on the molecular and rheological properties of starch. *Carbohydrate Polymers, 62*(3), 205–213.
Li, J., Kong, X., & Ai, Y. (2022a). Modification of granular waxy, normal and high-amylose maize starches by maltogenic alpha-amylase to improve functionality. *Carbohydrate Polymers, 290*, Article 119503.
Li, J., Kong, X., & Ai, Y. (2022b). Modification of granular waxy, normal and high-amylose maize starches by maltogenic α-amylase to improve functionality. *Carbohydrate Polymers, 290*, Article 119503.
Li, J., Li, L., Zhu, J., & Ai, Y. (2021). Utilization of maltogenic α-amylase treatment to enhance the functional properties and reduce the digestibility of pulse starches. *Food Hydrocolloids, 120*, Article 106932.
Liang, W., Blennow, A., Herburger, K., Zhong, Y., Wen, X., Liu, Y., & Liao, Y. (2021). Effects of supplemental irrigation on winter wheat starch structure and properties under ridge-furrow tillage and flat tillage. *Carbohydrate Polymers, 270*, Article 118310.

Liang, W., Ding, L., Guo, K., Liu, Y., Wen, X., Kirkensgaard, J. J. K., … Zhong, Y. (2023). The relationship between starch structure and digestibility by time-course digestion of amylopectin-only and amylose-only barley starches. *Food Hydrocolloids, 139*, Article 108491.

Liu, F., Antoniou, J., Li, Y., Ma, J., & Zhong, F. (2015). Effect of sodium acetate and drying temperature on physicochemical and thermomechanical properties of gelatin films. *Food Hydrocolloids, 45*, 140–149.

Luallen, T. (2018). Chapter 13 - utilizing starches in product development. In M. Sjöö, & L. Nilsson (Eds.), *Starch in food (second edition)* (pp. 545–579). Woodhead Publishing.

Maniglia, B. C., Castanha, N., Le-Bail, P., Le-Bail, A., & Augusto, P. E. (2021). Starch modification through environmentally friendly alternatives: A review. *Critical Reviews in Food Science and Nutrition, 61*(15), 2482–2505.

Song, Y., & Jane, J.-L. J. C. P. (2000). Characterization of barley starches of waxy, normal, and high amylose varieties. *Carbohydrate Polymers, 41*(4), 365–377.

Tian, Y., Liu, X., Kirkensgaard, J. J. K., Khakimov, B., Enemark-Rasmussen, K., Hebelstrup, K. H., … Zhong, Y. (2024). Characterization of different high amylose starch granules. Part I: Multi-scale structures and relationships to thermal properties. *Food Hydrocolloids*, 146.

Tian, Y., Petersen, B. L., Liu, X., Li, H., Kirkensgaard, J. J. K., Enemark-Rasmussen, K., … Blennow, A. (2024). Characterization of different high amylose starch granules. Part II: Structure evolution during digestion and distinct digestion mechanisms. *Food Hydrocolloids*, 149.

Tian, Y., Wang, Y., Liu, X., Herburger, K., Westh, P., Møller, M. S., … Blennow, A. (2023). Interfacial enzyme kinetics reveals degradation mechanisms behind resistant starch. *Food Hydrocolloids, 140*.

Wang, S., Wang, S., Guo, P., Liu, L., & Wang, S. (2017). Multiscale structural changes of wheat and yam starches during cooking and their effect on in vitro enzymatic digestibility. *Journal of Agricultural and Food Chemistry, 65*(1), 156–166.

Wurzburg, O. (1972). Starch in the food industry. In *Handbook of food additives, 2nd ed* (p. 998). Cleveland: CRC press.

Yang, P., Haken, A. E., Niu, Y., Chaney, S. R., Hicks, K. B., Eckhoff, S. R., … Singh, V. (2005). Effect of steeping with sulfite salts and adjunct acids on corn wet-milling yields and starch properties. *Cereal Chemistry, 82*(4), 420–424.

Zhai, Y., Li, X., Bai, Y., Jin, Z., & Svensson, B. (2022). Maltogenic α-amylase hydrolysis of wheat starch granules: Mechanism and relation to starch retrogradation. *Food Hydrocolloids, 124*, Article 107256.

Zhong, Y., Herburger, K., Kirkensgaard, J. J. K., Khakimov, B., Hansen, A. R., & Blennow, A. (2021). Sequential maltogenic α-amylase and branching enzyme treatment to modify granular corn starch. *Food Hydrocolloids, 120*, Article 106904.

Zhong, Y., Keeratiburana, T., Kain Kirkensgaard, J. J., Khakimov, B., Blennow, A., & Hansen, A. R. (2021). Generation of short-chained granular corn starch by maltogenic alpha-amylase and transglucosidase treatment. *Carbohydrate Polymers, 251*, Article 117056.

Zhong, Y., Li, Z., Qu, J., Bertoft, E., Li, M., Zhu, F., Blennow, A., & Liu, X. (2021). Relationship between molecular structure and lamellar and crystalline structure of rice starch. *Carbohydrate Polymers, 258*, Article 117616.

Zhong, Y., Tai, L., Blennow, A., Ding, L., Herburger, K., Qu, J., … Liu, X. (2022). High-amylose starch: Structure, functionality and applications. *Critical Reviews in Food Science and Nutrition*, 1–23.

Zhong, Y., Tian, Y., Liu, X., Ding, L., Kirkensgaard, J. J. K., Hebelstrup, K., … Blennow, A. (2021). Influence of microwave treatment on the structure and functionality of pure amylose and amylopectin systems. *Food Hydrocolloids, 119*, Article 106856.

Zhong, Y., Xu, J., Liu, X., Ding, L., Svensson, B., Herburger, K., Guo, K., Pang, C., & Blennow, A. (2022). Recent advances in enzyme biotechnology on modifying gelatinized and granular starch. *Trends in Food Science & Technology, 123*, 343–354.